Catalysis Today 232 (2014) 165–170

Contents lists available at ScienceDirect

Catalysis Today

journal homepage: www.elsevier.com/locate/cattod

Effect of a crystalline phase of TiO_2 photocatalysts on the photodeposition of Rh metal nanoparticles

Akira Yamamoto[a], Junya Ohyama[b,c], Kentaro Teramura[a,c,d,*], Tetsuya Shishido[c,e], Tsunehiro Tanaka[a,c,*]

[a] Department of Molecular Engineering, Graduate School of Engineering, Kyoto University, Katsura, Nishikyo-ku, Kyoto 615-8510, Japan
[b] Department of Applied Chemistry, Graduate School of Engineering, Nagoya University, Furo-cho, Chikusa-ku, Nagoya 464-8603, Japan
[c] Elements Strategy Initiative for Catalysts & Batteries (ESICB), Kyoto University, Kyotodaigaku Katsura, Nishikyo-ku, Kyoto 615-8520, Japan
[d] Precursory Research for Embryonic Science and Technology (PRESTO), Japan Science and Technology Agency (JST), Honcho Kawaguchi, Saitama 332-0012, Japan
[e] Department of Applied Chemistry, Tokyo Metropolitan University, Minami-Osawa, Hachioji, Tokyo 192-0397, Japan

ARTICLE INFO

Article history:
Received 16 July 2013
Received in revised form 5 September 2013
Accepted 18 September 2013
Available online 23 October 2013

Keywords:
Photodeposition
Photocatalyst
Crystalline phase
Rh nanoparticles
Dispersive XAFS

ABSTRACT

Effect of a crystalline phase of TiO_2 is investigated in the photodeposition processes of Rh metal nanoparticles on TiO_2 photocatalysts having anatase and rutile phase by means of in situ time-resolved energy dispersive X-ray absorption fine structure spectroscopy (DXAFS), transmission electron microscopy (TEM), and X-ray photoelectron spectroscopy (XPS). The important factor was neither its crystallite size nor its specific surface area, and was the crystalline phase. In situ time-resolved DXAFS analysis clarified that the Rh metal nanoparticles with a uniform size appear on both anatase and rutile phases of TiO_2, whereas the appearance rate of Rh metal nanoparticles decreases with the photoirradiation time only on the rutile phase of TiO_2. The TEM observation and XPS depth analysis revealed that the bare surface of photodeposited Rh metal nanoparticles on the rutile is exposed, although that on the anatase is partially covered with TiO_2 due to strong metal-support interaction (SMSI) between Rh metal nanoparticle and $TiO_{2-\delta}$.

1. Introduction

It has widely been recognized that the photodeposition, which Bard and co-worker have reported in 1978 [1], is a very valuable method to recover of noble metals [2–4], to remove metal cations from aqueous effluent [5–7], and to prepare metal-supported catalysts [8,9] and metal-promoted photocatalysts [10–13]. Photoexcited electrons in a photocatalyst reduce metal cations that have more positive reduction potential than the conduction-band level of the photocatalyst. The simultaneously generated holes in the valence band are consumed with oxidation of a reactant such as alcohol, aldehyde, or carboxylic acid [1,5]. In the several studies, it is found that the metal species were photodeposited on specific sites on a photocatalyst, for example, an edge or plane of a photocatalyst crystallite [14–16]. Interestingly, the morphology of the resulting metal nanoparticles greatly varies among the kinds of photocatalyst. These phenomena inspire us to study the systematic kinetics and mechanism for the formation of nanoparticles as well as the structure of resulting metal species. X-ray absorption fine structure (XAFS) spectroscopy is a powerful method to elucidate the formation process of the metal nanoparticles and reactivity of surface species [17–22]. Fernandez et al. have observed the photodeposition of Au nanoparticles by an in situ XAFS measurement, where the suspension composed of an Au precursor and TiO_2 was pumped out from the photochemical reactor to the XAFS measurement cell under photoirradiation [23,24]. We have also successfully observed the photodeposition process of Rh metal nanoparticles on TiO_2 using in situ time-resolved energy dispersive X-ray absorption fine structure spectroscopy (DXAFS), and proposed unique particle-formation mechanism that Rh metal nanoparticles with a uniform size constantly appear one after another on the surface of TiO_2 [25,26]. We have also successfully observed the formation process of Rh and Au nanoparticles by means of time-resolved Quick XAFS experiments [27–31].

Recently, we reported that photodeposited Rh and Pt metal nanoparticles on TiO_2 (JRC-TIO-8, anatase) were modified with $TiO_{2-\delta}$ which is well-known as a key species in the strong metal-support interaction (SMSI) [32,33]. Generally, the SMSI can be observed when group VIII noble metals (e.g., Pt, Rh, Pd, and Ir) on reducible oxide supports (e.g., TiO_2 and Nb_2O_5) are treated

---

* Corresponding authors at: Department of Molecular Engineering, Graduate School of Engineering, Kyoto University, Kyotodaigaku Katsura, Nishikyo-ku, Kyoto 615-8510, Japan. Tel.: +81 75 383 2562; fax: +81 75 383 2561.
E-mail address: teramura@moleng.kyoto-u.ac.jp (K. Teramura).

0920-5861/$ – see front matter. Crown Copyright © 2013 Published by Elsevier B.V. All rights reserved.
http://dx.doi.org/10.1016/j.cattod.2013.09.024

with H_2 at high temperature and causes the modification of metal nanoparticles with reduced supports (e.g., $TiO_{2-\delta}$) generated by H_2 treatment. It is both interesting and incredible that the SMSI take places by photoirradiation at room temperature as well as by H_2 treatment at high temperature. Most probably, $TiO_{2-\delta}$ generated by the photoirradiation of TiO_2 cause the modification and the disorganized structure of Rh and Pt metal nanoparticles. Amount, type and property of $TiO_{2-\delta}$, therefore, may have an effect on the SMSI in the photodeposition process. Li et al. reported that the SMSI occurs by H_2 reduction at lower temperature on anatase TiO_2 than on rutile [34], suggesting that the crystalline phase of TiO_2 photocatalysts affects the interaction of Rh metals and TiO_2. In this study, we investigated the photodeposition processes of Rh metal nanoparticles on TiO_2 photocatalysts having anatase and rutile phases, and their structure by means of in situ time-resolved DXAFS spectroscopy, XPS with sputtering, TEM observation.

2. Experimental

2.1. Materials

TiO_2 samples used in this study (JRC-TIO-1, 3, 6, 8, and 10) were kindly supplied from the Japan Catalysis Society. All the samples were calcined in air at 673 K for 3 h before use. Crystalline phase of each TiO_2 was determined by X-ray diffraction technique (XRD). The crystallite size was estimated by the use of the Scherrer's equation. The specific surface area of sample was determined using N_2 adsorption isotherm at 77 K. Crystalline phases, surface areas, and crystallite sizes of TiO_2 used in this study were listed in Table S1 of the supplementary data. In this paper, for simplicity, we denote the phase and the catalyst like **N**–**X** where **N** is the catalyst name JRC-TIO-**N**, and **X** is **A** or **R** meaning anatase or rutile, respectively; i.e., JRC-TIO-8 (anatase) to **8-A** and JRC-TIO-3 (rutile) to **3-R**.

2.2. Photodeposition

The photodeposition of Rh nanoparticles on TiO_2 was carried out in a closed batch system. As a typical photodeposition method, 500 mg of TiO_2 was suspended in 3.2 mL of methanol in a batch reactor made of Pyrex glass with a flat ceiling window for irradiation, followed by the addition of 0.8 mL of an aqueous solution of $RhCl_3$ (Wako Pure Chemical Industries, Ltd., 0.076 mmol of Rh). The suspension was irradiated with a 200 W Hg-Xe lamp equipped with fiber optics, a collective lens, and a mirror (San-Ei Electric Co., Ltd., UVF-204S type C) after N_2 bubbling for 10 min. Then the suspension was filtered, and the residual powder was washed with 100 mL of purified water and was placed in an oven at 353 K.

2.3. Time-resolved dispersive XAFS measurements

In situ time-resolved DXAFS measurements at the Rh-K edge (~23.2 keV) were performed at the BL28B2 beamline of the SPring-8. The DXAFS measurement system consists of a polychromator set to a Laue configuration with a Si (4 2 2) net plane and a position-sensitive detector (PSD) mounted on a θ–2θ diffractometer [25,27]. The X-ray energy was calibrated by the spectrum of a Rh foil. The above-mentioned Pyrex reactor with the suspension was set at the X-ray focal spot. Light irradiation of the reactor was synchronized with exposure to X-rays. The exposure time of the PSD was 249 ms. Fifty shots were accumulated; 12.45 s per a spectrum. We programmed the collection of 500 snapshot spectra (124.5 s) in the dark and then 7000 snapshot spectra (1743 s) under photoirradiation consecutively. The measurement program was repeated four times to obtain the spectral change at 116.2 min under photoirradiation. Analysis of XAFS spectra was performed using the REX2000 program (version 2.5.9, Rigaku Corp.). The k^3-weighted EXAFS oscillation in the range of 2.78–10.7 Å was Fourier-transformed.

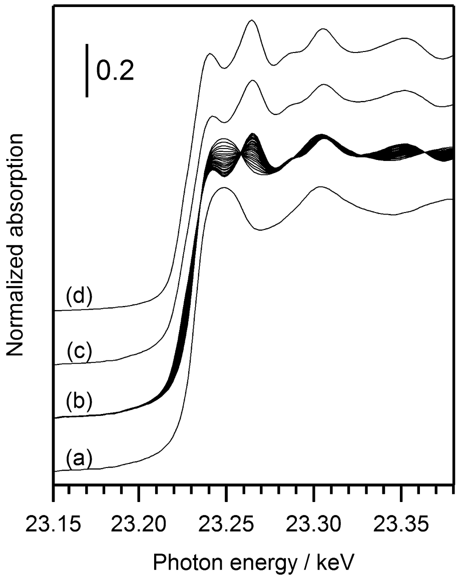

Fig. 1. XANES spectra at the Rh-K edge of reference samples and the suspension consisting of a methanol aqueous solution of $RhCl_3$ and **3-R**: (a) before irradiation, (b) under irradiation, (c) after irradiation for 116 min, and (d) Rh foil.

2.4. Characterization

XPS spectra were acquired using an ULVAC PHI 5500MT system. Samples mounted on indium foil were analyzed using Mg $K\alpha_{1,2}$ radiation (15 kV, 400 W) in a vacuum chamber ($<1 \times 10^{-8}$ Torr). The electron takeoff angle was set at 45°. Binding energies were referenced to C 1s peak of residual carbon at 284.6 eV. Sputtering was performed by a Xe ion beam (3.0 kV) with raster size 1.1 mm × 2.1 mm. TEM, STM, and EDX mapping images were obtained with a JEOL JEM-2100F transmission electron microscope operating at an accelerating voltage of 200 kV. TEM samples were prepared by depositing drops of a methanol suspension containing small amounts of the powders onto a carbon-coated copper grid (Okenshoji Co., Ltd.).

3. Results and discussion

3.1. XANES spectra

Fig. 1 shows a series of Rh-K edge XANES spectra of the suspension comprised of a methanol aqueous solution of $RhCl_3$ and **3-R** under photoirradiation. The edge energy of XANES shifted to lower photon energy with the elongation of photoirradiation time. The XANES spectrum after 116 min of photoirradiation was almost identical to that of the Rh foil. This result indicates that Rh^{3+} ions are reduced to Rh^0 metals by photoirradiation. There is no change in the spectrum from $RhCl_3$ without TiO_2 or photoirradiation. The XANES spectral change corresponding to the reduction of Rh^{3+} ions to Rh^0 metals exhibits the isosbestic points, which indicates that Rh^{3+} ions are reduced to Rh^0 metals without any intermediates within the measurable time. All the Rh-K edge XANES spectra can be represented with the linear combination of the two XANES spectra; one is that of Rh^{3+} ions in the initial state and the other is that of Rh^0 metals in the final state. The least-squares fitting of each XANES spectrum with the linear combination allowed us to obtain the fractions of the Rh^0 metals and Rh^{3+} ions using **3-R** and **8-A** as shown in Fig. 2. The fraction of Rh^0 metals increased with the